Experimental study on flow structure in riffle-pool channels

Like Li, Niannian Fan* and Xingnian Liu

State Key Laboratory of Hydraulics and Mountain River Engineering, College of Water Resource & Hydropower, Sichuan University, China

*Corresponding author: fannian7172@126.com

Abstract: Because of the riverbed evolution and geological tectonics, the river geometry has changed obviously, forming a wide and narrow alternated channel .The area with shallow water depth is easy to form riffles. The area with narrow deep water often forms deep pools. Flow rate will increase or decrease. The hydraulic characteristics of riffle-pool with clear water scouring under steady state were studied by using three-dimensional overlooking acoustic Doppler velocimeter (ADV：Nortek-vectrino II), a camera, a underwater high-speed camera and a laser rangefinder . The results showed that with the change of channel geometry, the water level of cross-section would change accordingly; logarithm law could well describe the time-averaged velocity distribution near the wall. However, the bed morphology affected the flow structure near the bed to a certain extent; because of the irregular cross-section and the influence of the bed topography, the cross-section gradually changed. The Reynolds stress varied significantly in the area where the cross-section decreased gradually, indicating that the water body had strong shearing action. In the enlarged area, the Reynolds stress distributed uniformly.

1. Introduction

Due to the development of the riverbed and the impact of geological structures, the geometry of the river channel is obviously changed to form a wide and narrow river channel. The water depth in the wide area is shallow, and it is easy to form a shoal. The water depth in the narrow part is deep, often forming a deep pool, and the flow rate will increase or decrease with the depth. The slope of the riffle-pool is generally less than 0.02, which is usually a straight or curved gravel riverbed river. Usually, the distance between the deep pools is 5-7 times to the width of the river, but if there are a large number of collapsed trees in the river, its distance will become smaller [1].

Since the riverbed gradient in the trailing edge area of the deep pool is larger than that of the water surface, the water flow will spread in the vertical direction. Many scholars at home and abroad have conducted extensive research on this wide and narrow river channel. Nelson et al. (2015) studied the geomorphic dynamic response of gravel rivers with varying river widths to sediment transport changes through a sink test. The change does not affect the location and topography of the shoal-deep pool. The river channel responds to changes in sediment recharge by adjusting the gradient [2]. MacVicar and Best (2013) generalized the bed surface morphology of smooth deep pools and shoals with smooth boundaries using perturbation theory, pointing out that the shear velocity and Gaussian wake parameters are not sensitive to the adjustment of river width, while the concentration of lateral flow is The recovery of the main Reynolds stress can be described by two-stage propagation and a relaxation response that varies with the width of the river [3]. Yan et al. (2011) analyzed the local head loss characteristics of the river wide expansion section affected by water depth shrinkage based on

laboratory tests [4]. Zhou et al. (2013) established a two-dimensional flow model of a wide and narrow river channel in a mountainous area to simulate the characteristics of water flow motion [5]. Caamaño et al. (2012) established a generalized model to explain the characteristics of the water flow structure of the riffle-pool in the gravel river and how to respond to the change of external force through detailed measurement and simulation of the three-dimensional water flow structure [6]. MacVicar and Roy (2007) studied the distribution of the velocity and turbulence intensity of the riffle-pool forced by the tree blocking channel, pointing out that the deceleration and acceleration flow generated by the expansion and contraction in the vertical direction can explain many observations [7]. Papanicolaou and Elhakeem (2007) combined with field measurements and experiments, pointed out that due to the change of the section shape of the channel. The average shear stress does not approximate the magnitude of the fluid shear stress [8]. Hoan et al. (2007) believe that the turbulence intensity and Reynolds stress distribution deviate from the theoretical and experimental curves of uniform flow due to the irregular geometry of the river [9]. Venditti et al., (2014) used the Acoustic Doppler Velocity Profiler (ADCP) to measure the Fraser Canyon in Canada. When the water flowed into the canyon, high-speed water flowed near the bed and low-speed water flowed on the surface, causing a reversal of speed. The water then surges along the side walls of the canyon, creating a counter-rotation that causes the main stream to deviate from the center of the river [10]. Yang et al., (2007) investigate the variation of different resistance coefficients with the stage use symmetric compound channel with a large bed roughness and summarize different representative methods for assessing the composite roughnesses in compound channels [11].

Due to the turbulent flow, the kinetic transfer of the bed, and the obvious feedback relationship between the bed surface micro-topography [12], Carbonneau and Bergeron (2000) pointed out through experiments that the bed load will change the dissipation rate of turbulent kinetic energy, and thus affect the near-bed area. Flow rate distribution [13]. In the past, the experimental study on the wide and narrow phase water channel was mostly fixed bed surface [3-5], and it was rarely concerned about the water flow structure under the condition of clear water scouring. This paper aims to study the water flow under the steady state of wide and narrow rivers through the sink test. The study of flow structure can improve the understanding of the type of river in the shoal-deep pool.

2. Experimental materials and settings

The test was conducted at the University of British Columbia, Canada, with a test tank length of 18 m and a trough-wide gradient sink with a width of 0.8 m and a narrowest point of only 0.38 m. The initial slope of the sink is 0.015 and the flow rate is 50 L/s. The test is divided into six stages: clear water flushing, stable sanding, clear water flushing, increasing water flow, increasing water flow again and adding fine particles. At the beginning of the test, the sand was first laid flat at the bottom of the tank. The particle size distribution of the sand before and after the test is shown in Figure 1. The water is then flushed and the airfoil is mounted on the connecting rod of the three-dimensional overhead acoustic Doppler velocimetry and the underwater camera to reduce wake. During the test, there was no sand in the upper reaches, and the sediment transported by the water flow originated from the bed surface. After 78 hours of clean water flushing, the sediment transport rate at the exit section has been very small, dropping to 0.075 g/s, falling below the maximum sediment transport rate of 7.55 g/s (one hour average sediment transport rate). The bottom of the sink has also been shaped into a certain shape of the bed. It is washed out of the deep pool at the narrow position of the river, and is stacked into a shallow beach at the widened position of the river, as shown in Figure 2. At this time, the cross-sectional flow velocity was measured using ADV, and the surface morphology information was collected using a camera and a laser topographic scanner. This paper mainly studies the water flow structure when the bed surface is in a stable state after 78 hours of water washing.

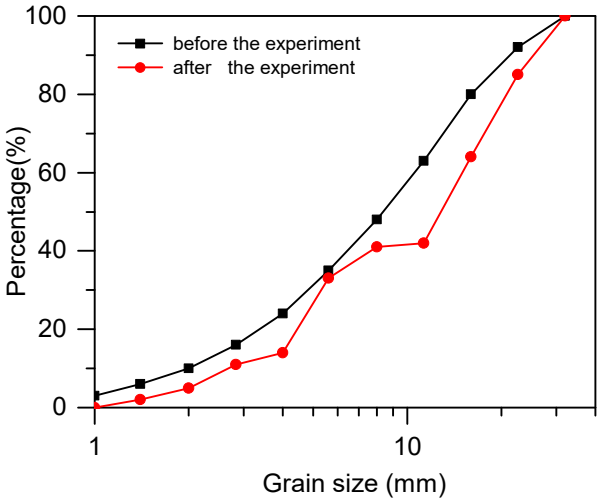

Fig. 1 Grain size distribution

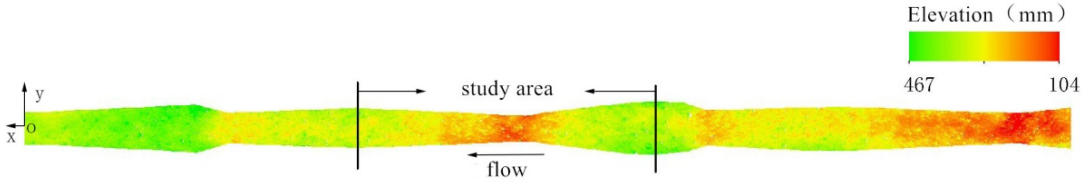

Fig. 2 Bed topography

The test tank has three wide and narrow river sections. In order to avoid the influence of the inlet and outlet water flow, the middle section of the tank is selected as the study area. A total of 17 measuring sections are set in this area, the 1 # section is set at x= -5.6 m, the 17 # section is set at x= -10 m, and the specific arrangement of the measuring section is shown in Fig. 3. According to the change of the geometry of the water tank, measuring sections with unequal spacing and different numbers of measuring vertical lines are set, and each vertical line has different number of measuring points due to the difference of water depth. The arrangement of specific measuring points is shown by the dashed line in Figure 3. The single short line segment in each broken line represents a measuring section in the longitudinal direction to explore the water flow structure of the wide and narrow phase channel in detail. The instrument measures the instantaneous velocity of the non-uniform flow on the lateral boom overlooking the ADV. The instrument measures the flow of water at 4～7.4 cm below the bottom of the probe. The sampling frequency and time are set to 50 Hz and over 40 seconds respectively. The number of sampling points in each measurement period is greater than 2000, which has a high signal-to-noise ratio and correlation. Despikng of ADV data is performed by Derek G. Goring [14].

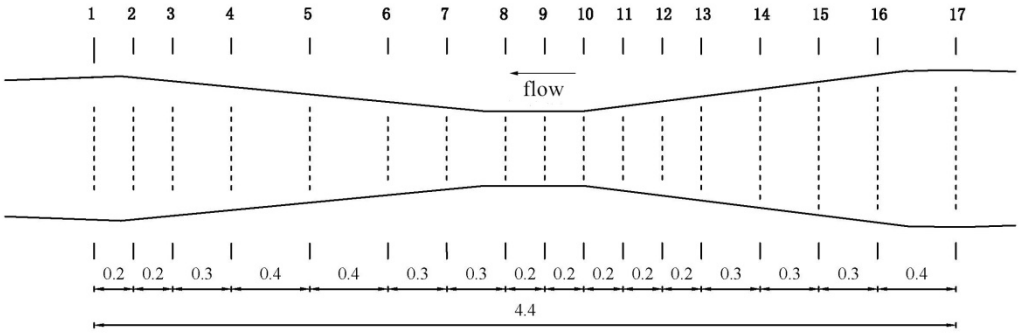

Fig. 3 Test measurement section layout (m)

3. Results and analysis

3.1 Water depth changes along the river

Figure 4 shows the distribution of water depth along the course. As the geometry of the channel changes, the water level changes relatively small. Due to the narrowness of the channel, the deep water was washed out, and the water depth increased significantly. After that, the river was widened and piled up into shoals, and the water depth began to gradually decrease. It can be seen from the figure that the minimum water depth does not correspond to the widest part of the section, but occurs at the position of x= -6.3 m (4 #section); the maximum depth of water does not correspond to the narrowest part of the section, but occurs at x = -7.9 m (9 #section) position, 9 # section is also the lowest point of the bed, combined with Figure 2 can be found that this position is the most severe.

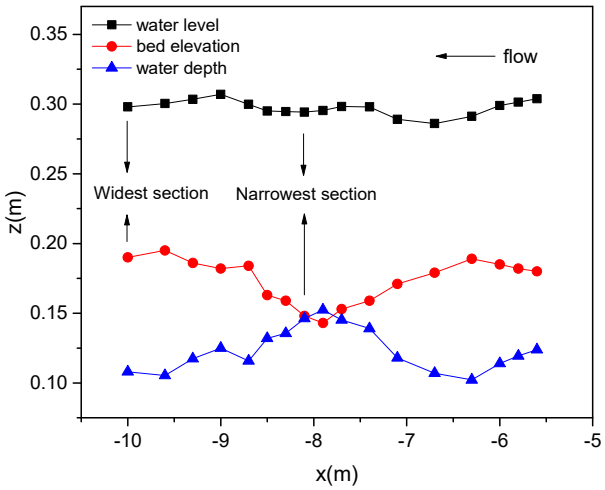

Fig. 4 Water depth changes along the river

3.2 Vertical distribution of time averaged velocity

During the flow of water in the tank, the flow velocity distribution is not uniformly affected by the geometry of the channel and the morphology of the bed. Generally, the flow velocity in the lateral direction increases from the boundary of the sink to the intermediate position, and increases in depth along with the increase in depth. We used the ADV flow meter to measure the water flow rate from the diverging to the tapered section at different depths from the riverbed.

According to the previous study of the time-averaged velocity distribution of uniform flow and non-uniform flow [15-20], in order to study the turbulence characteristics, the velocity distribution is fitted to the turbulent region following the logarithmic distribution ($h/z \leqslant 0.2$). The outlet section of the experimental tank can be approximated as a uniform flow. Since the frictional velocity u^* of the non-uniform flow is very difficult to determine, in order to simplify the calculation, the frictional flow velocity u^* of the outlet section is assumed to be 0.046 m/ s. The longitudinal velocity of all sections is normalized by using the frictional velocity u^* as a general parameter. The instantaneous velocity of each point measured by the ADV is arithmetically averaged to obtain the average flow velocity value of the point on the vertical line. The calculation formula is:

$$u^+ = \frac{u}{u^*} \tag{1}$$

$$y^+ = \frac{yu^*}{v} \tag{2}$$

In the formula, u: the average flow velocity along the vertical direction, v: the kinematic viscosity of the water, y: the distance from the measurement point to the bed surface. See Figure 5 below for the change in flow velocity from the gradually expanding section to the tapered section.

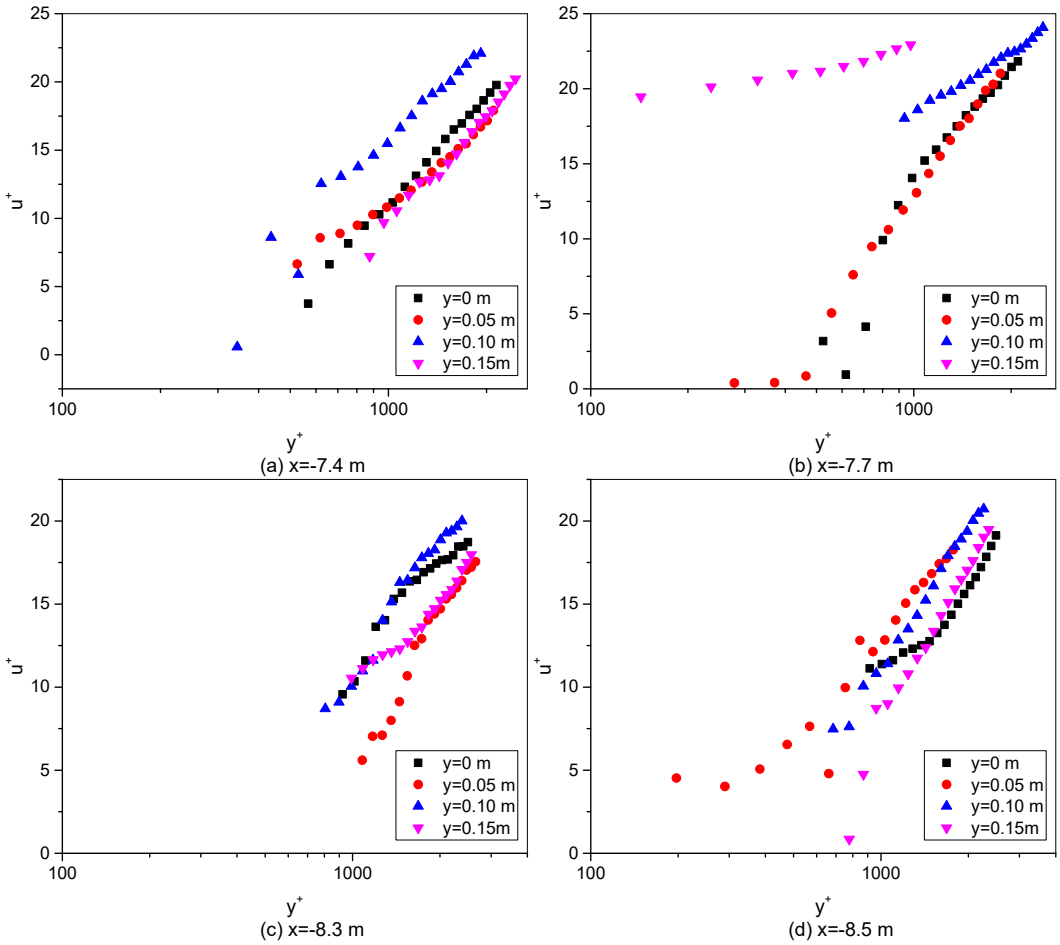

Fig. 5 Time-averaged velocity distribution

It is obvious from the figure that all the velocity profiles are basically in line with the logarithmic distribution, which is consistent with the previous research results of non-uniform flow [21].

3.3 Reynolds stress

The Reynolds stress reflects the momentum transfer caused by the pulsation of the water flow. According to the pulsation speeds u', v' and w' of the water flow in the x, y and z directions, the Reynolds stress of the XOY and XOZ planes is calculated by the pulsation correlation method, and the Reynolds stress is obtained. The stress is normalized by u^{*2}, and the distribution of the dimensionless Reynolds stress along the vertical direction can be obtained. The component of the dimensionless Reynolds stress has anisotropy in the vertical and lateral directions, and the distribution from the divergent section to the tapered section along the groove width is shown in Figure 6.

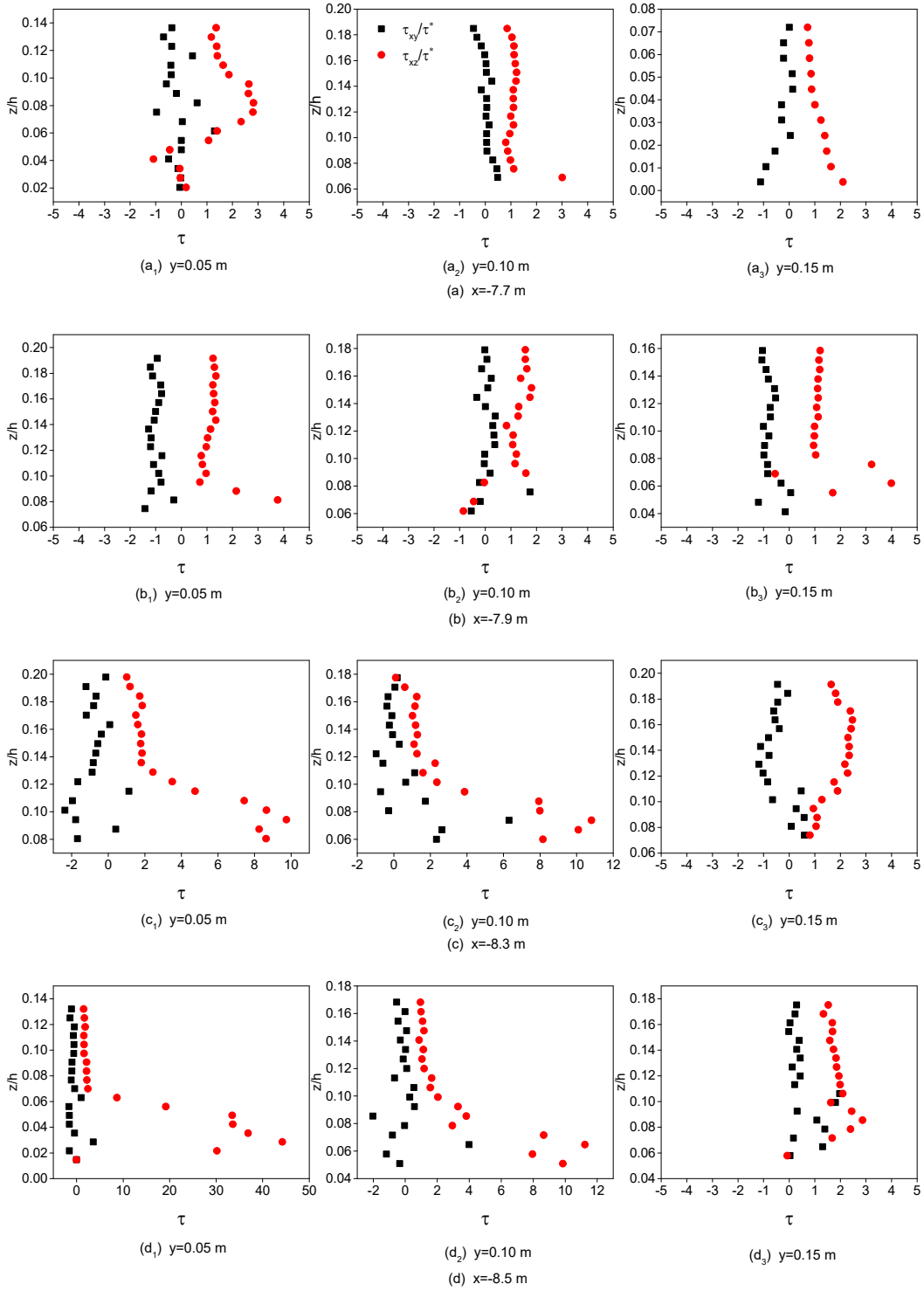

Fig. 6 Typical section Reynolds shear stress distribution

Overall, the Reynolds stress has a higher value near the bed surface, indicating that turbulence is due to wall shear. The difference of shear stress in vertical and horizontal directions is obvious. With the increase of water depth, the influence of bed surface is gradually weakened. The difference between τ_{xy} and τ_{xz} gradually becomes smaller. In the tapered section, about 0.12 h water depth, Renault The stresses τ_{xy} and τ_{xz} are hardly affected by the morphology of the bed surface and tend to

be parallel along the vertical direction. In the divergent section, the influence of the bed surface shape extends only to the depth of 0.08 h.

The value of τ_{xy} is relatively stable, and the fluctuation range is relatively small. The section x= -7.7 m and x= -8.5 m are relatively far from the narrowest position of the water tank, and are relatively less affected by the geometry of the water tank. Nearby, and the section x= -7.9 m and x= -8.3 m, the channel geometry changes significantly, τ_{xy} deviates from the value of 0, and fluctuates roughly between 1 and -1.

The fluctuation range of τ_{xz} is relatively large. τ_{xz} is affected by the riverbed topography on the near riverbed surface, and the Reynolds stress fluctuation is abnormally significant, especially for the area where the section is gradually reduced. It can even reach several times the area where the section is gradually enlarged (section x= -7.7 m and x= -7.9 m), indicating that the shearing effect of water in this area is very strong.

4. Conclusion

This paper focuses on the water flow structure under the steady state of water flushing between wide and narrow rivers, and draws the following conclusions:

1. The water level is less affected by the geometry of the river channel, and there is no obvious change. The minimum water depth of the tank corresponds to the lowest point of the bed surface, indicating that the location is the most severe.
2. The time-averaged velocity distribution of the vertical direction of different water depths of each section is studied. It is found that the logarithm law is not only applicable to the near-wall area of the open channel uniform flow, but also can better describe the turbulent flow area of the open channel under the condition of wide and narrow river channel clear water scouring. The distribution of average speed. The average flow velocity near the bed surface does not conform to the logarithmic distribution, and the shape of the bed surface affects the water flow structure near the riverbed surface to some extent.
3. The Reynolds stress fluctuation of the near wall surface is large, and the water body has strong shearing effect. With the increase of water depth, the Reynolds stress is less affected by the shape of the bed surface, and the difference between τ_{xz} and τ_{xy} is smaller. Due to the influence of the channel geometry, the τ_{xy} and τ_{xz} are almost unaffected by the shape of the bed surface in the tapered section, which is almost independent of the water depth of the bed. The distribution along the vertical line tends to two parallel lines, while in the divergent section; the influence only extends to the depth of 0.08 h.

References

[1] Montgomery, D. R., & Buffington, J. M. (1997). Channel-reach morphology in mountain drainage basins. Geological Society of America Bulletin, 109(5), 596-611.
[2] Nelson, P. A., Brew, A. K., Morgan, J. A. (2015). Morphodynamic response of a variable-width channel to changes in sediment supply. Water Resources Research, 51(7), 5717-5734.
[3] MacVicar, B., & Best, J. (2013). A flume experiment on the effect of channel width on the perturbation and recovery of flow in straight pools and riffles with smooth boundaries. Journal of Geophysical Research: Earth Surface, 118(3), 1850-1863.
[4] Yan, X. F., Yi. Z. J., Liu, T. H. et al.. (2011). Flow structure and characteristics of local head loss in transition channel. Journal of Yangtze River Scientific Research Institute.
[5] Zhou, S. F, Yi, Z. J, Yan, X. F. et al. (2013). Two-dimensional numerical simulation of flows in wide and narrow alternated channels in mountainous areas. Advances in Science and Technology of Water Resources, 33(01):22-26.
[6] Caamaño, D., Goodwin, P., Buffington, J. M. (2012). Flow structure through pool-riffle sequences and a conceptual model for their sustainability in gravel-bed rivers. River research and applications, 28(3), 377-389.
[7] MacVicar, B. J., & Roy, A. G. (2007). Hydrodynamics of a forced riffle pool in a gravel bed river:

1. Mean velocity and turbulence intensity. Water Resources Research, 43(12).
[8] Papanicolaou, A. N., & Elhakeem, M. (2007). Turbulence Characteristics in a Gradual Channel Transition. In World Environmental and Water Resources Congress 2007: Restoring Our Natural Habitat (pp. 1-6).
[9] Hoan, N. T., Booij, R., Stive, M. J. et al. (2007). Decelerating open-channel flow in a gradual expansion. In Asian and Pacific Coasts Conference, September 21-24, 2007, Nanjing, China. APAC.
[10] Venditti, J. G., Rennie, C. D., Bomhof, J. et al. (2014). Flow in bedrock canyons. Nature, 513(7519), 534.
[11] Yang, K. J., Cao, S. Y., Liu, X. N. (2007). Flow resistance and its prediction methods in compound channels. Acta Mechanica Sinica, 23(1), 23-31.
[12] Naden, P. S. (1988). Models of sediment transport in natural streams. Modelling Geomorphological Systems. John Wiley and Sons New York. 1988. p 217-258, 13 fig, 6 tab, 86 ref.
[13] Carbonneau, P. E., & Bergeron, N. E. (2000). The effect of bedload transport on mean and turbulent flow properties. Geomorphology, 35(3), 267-278.
[14] Goring, D. G., & Nikora, V. I. (2002). Despiking acoustic doppler velocimeter data. Journal of Hydraulic Engineering, 128(128), 117-126.
[15] Wang, S. Y., Zhou, S. F., Zhao, X. E. (2013). Experimental study on the flow characteristics at local diverging-converging sections in mountain lotus root shape channel. Journal of Sichuan University, 45, 51-54.
[16] Liu, C. J, Li, D. X, Wang X. K. (2005). Experimental study on friction velocity and velocity profile of open channel flow. Journal of Hydraulic Engineering, 36(8), 0950-0955.
[17] Afzalimehr, H., & Anctil, F. (1999). Velocity distribution and shear velocity behaviour of decelerating flo. Canadian Journal of Civil Engineering,26(26), 468-475.
[18] Balachandar, R., Hagel, K., & Blakely, D. (2002). Velocity distribution in decelerating flow over rough surfaces. Canadian Journal of Civil Engineering, 29(2), 211-221.
[19] Wang, X. K, Yi Z. J., Yan X. F. et al. (2015). Experimental study of the flow structure of decelerating and accelerating flows under a gradually varying flume. Journal of Hydrodynamics. B27(3), 340-349.
[20] Liu, C., Wright, N., Liu, X., Yang, K. (2014). An analytical model for lateral depth-averaged velocity distributions along a meander in curved compound channels. Advances in Water Resources, 74, 26-43.
[21] Wang, J. J., & Dong, Z. N. (1996). Open-channel turbulent flow over non-uniform gravel beds. Applied Scientific Research, 56(4), 243-254.